Non-reversible Monte Carlo: an example of "true" self-repelling motion

A. C. Maggs

E-mail: anthony.maggs@espci.fr
CNRS UMR 7083, ESPCI Paris, Université PSL, 10 rue Vauquelin, 75005 Paris, France.

Abstract. We link the large-scale dynamics of non-reversible Monte Carlo algorithms as well as a lifted TASEP to an exactly soluble model of self-repelling motion. We present arguments for the connection between the problems and perform simulations, where we show that the empirical distribution functions generated from Monte Carlo are well described by the analytic solution of self-repelling motion.

Introduction

Non-reversible Monte Carlo sampling as developed for hard disks [1], and its generalisation to arbitrary potentials [2, 3, 4] has many wonderful properties which facilitate the equilibration of large complex systems faster than conventional Monte Carlo, or molecular dynamics algorithms [5, 6]. Such Monte Carlo methods do not implement the historic choice of detailed balance, rather the weaker condition of global balance. This leads to much greater freedom of choice for the implementer of algorithms. However, analytic understanding of the large-scale, effective dynamics is lacking. This is in strong contrast to, for instance, molecular dynamics which generate the Navier-Stokes equations at large scales in a fluid. Extensive theoretical analysis of the mode structure of these hydrodynamic equations gives us the slow hydrodynamic modes of sound, vorticity and heat propagation, which limit the large-scale sampling of a fluid.

What are the equivalent statements for event-chain Monte Carlo? What are the slow, hydrodynamic modes? This letter aims to present the continuum, coarse-grained equations describing event-chain simulation and demonstrate their equivalence to an exactly soluble model of a growing polymer. Clearly, if one understands the temporal evolution of the coarse-grained equations, it will be possible to make exact statements on the evolution of densities and correlations, and perhaps find better implementations in the future. The present letter makes a direct link between event-chain Monte Carlo simulation and "true" self-repelling motion, [7] which has been much studied using a variety of physical methods including scaling [8, 9] and renormalisation [10]. Recently this model has been studied using advanced methods based on interacting Brownian paths, which have led to exact, analytic results for the dynamical properties [11, 12, 13].

In this letter, we introduce the self-avoiding model, together with the exact results for its time evolution. We then summarise the behaviour of a class of non-reversible

algorithms before arguing that there is a link between these two dynamical systems. Finally, we present numerical evidence as to the identity of distribution functions with data coming from event-chain simulation of harmonic chains, as well as simulation of a lifted TASEP (Totally Asymmetric Simple Exclusion Process).

True self-avoiding motion

The "true" self-avoiding walk was introduced, [7] as a dynamic model of polymer growth, in contrast to an equilibrated statistical ensemble of equilibrated polymers. On a lattice, monomers are added successively to a chain, trying to avoid places where the polymer has already passed. The probability of choosing a site i, which has been visited $L_i(t)$ times is then

$$p_i(t+1) = \frac{e^{-\lambda L_i(t)}}{\sum_j e^{-\lambda L_j(t)}} \tag{1}$$

Where the sum is over all neighbours j of the current position at time t. $\lambda > 0$ measures the strength of the repelling interaction. The model has infinite memory, required to calculate the placement probabilities of the new monomer. The large-scale behaviour of the process is believed to be independent of λ for finite values of the parameter.

It was argued, [7] that this dynamic process has a continuum limit so that the effective, large-scale behaviour is of the form

$$\frac{d\mathbf{X}(t)}{dt} = -\nabla L(t, \mathbf{X}(t)) + \xi(t) \tag{2}$$

$$\frac{dL(t,\mathbf{x})}{dt} = \delta(\mathbf{x} - \mathbf{X}(t)) \tag{3}$$

The function, $L(t, \mathbf{x})$, a *local time*, cumulates memory as to the occupation of the position $\mathbf{X}(t)$. It is the continuum analogue of the discrete variable L_i of eq.(1). We use the symbol L for the both the discrete and continuum variables. $\xi(t)$ in the formulation [7] corresponds to Gaussian noise. The growth of the end of the growing polymer is then repelled by regions where $L(t, \mathbf{x})$ has become large, in a manner which is analogous to the original lattice model. This continuum model is amenable to many of the formal methods of field theory [14, 10].

Distributions functions of the model

Remarkably, the equations (2, 3) in one dimension lead to an explicitly solvable model [12, 13] involving time scaling in $t^{2/3}$ or $t^{1/3}$ for distribution functions; the Langevin-like eq. (2), does not lead to Brownian scaling in $t^{1/2}$. The exact solutions displayed in [13] show that two important distributions of physical variables exhibit scaling forms:

$$\rho_1(t, x) = t^{-2/3}\nu_1(xt^{-2/3}) \tag{4}$$

$$\rho_2(t, h) = t^{-1/3}\nu_2(ht^{-1/3}) \tag{5}$$

$\rho_1(t, x)$ is the distribution of displacement of the process after time t; in the original polymer problem of [7] it is the distribution of end-to-end separations. $\rho_2(t, h)$ is the

distribution of $h(t) = L(t, X(t))$, the density of previous visits to the endpoint of the polymer. The scaling functions are

$$\nu_1(x) = \sum_{k=1}^{\infty} \frac{p_k}{2} \delta'_k f_{2/3}(\delta'_k |x|) \tag{6}$$

$$\nu_2(h) = \frac{2 \cdot 6^{1/3} \sqrt{\pi}}{\Gamma(1/3)^2} e^{-(8h^3)/9} U(1/6, 2/3, (8h^3)/9) \tag{7}$$

$f_{2/3}(x)$ is the Mittag-Leffler function. δ'_k and p_k are calculated from the k'th zero of the derivative of an Airy function [13], U is a confluent hypergeometric function of the second kind [15]. The two functions eq. (6, 7), are rather distinctive visually and are far from Gaussian. They are plotted, in red, in Figs. 1, 2 .

Scaling argument for motion

A scaling argument [9], allows one to find the exponents describing the solutions. Let motion occur on the length scale t^α in time t. Then L must be of the form

$$L(t, x) \sim t^{(1-\alpha)} g(x/t^\alpha) \tag{8}$$

with an unknown scaling function $g(x)$. The driving force from eq. (2), $-\nabla L(t, x)$, then scales as $t^{(1-2\alpha)} g'(x/t^\alpha)$. If this force acts over the time t, it generates motion $\sim t^{(2-2\alpha)}$. It is natural that this motion is comparable to the total extent of the motion, t^α, so $t^{(2-2\alpha)} = t^\alpha$, and $\alpha = 2/3$.

Event-Chain Monte Carlo

Non-reversible, event-chain Monte Carlo methods are lifted variants of reversible Monte Carlo, where a single "active" particle is mobile, and at (to be determined) event times transfers motion to another particle, thereby avoiding the rejection step of reversible Monte Carlo methods [16]. We here consider event-chain algorithms suitable for simulation of models with continuous potentials [2, 4].

The total energy function is broken into a sum of "factor potentials". Each of these factors is then able to veto the motion of the active particle when a stochastic criterion, is violated. Vetos in the formulation of non-reversible Monte Carlo correspond to moment when a classical reversible algorithm would generate a rejection. At the moment of veto, motion then transfers to another particle allowing forward motion to continue. In the case of the sampling of a chain, each particle is in direct interaction with its two neighbours, the factor potentials are then just the contribution of each bond to the total energy; on a veto event the activity jumps to one of the two neighbours.

Particularly exciting results for event-chain simulation were found for low-dimensional XY spins [17] where it was argued that in one dimension the dynamics are characterized by a dynamic exponent, $z = 1/2$. This exponent links the relaxation time τ (in sweeps) of a system N spins via $\tau \sim N^z$. This result is smaller (hence, better) than is found in conventional reversible Monte Carlo or molecular dynamics where one finds $z = 2$ or $z = 1$. This exceptional scaling was generalized to more general models, including hard spheres and Lennard-Jones chains where a detailed study of the dynamics was performed [18]. As noted in [18], a dynamic exponent of $z = 1/2$, requires that the motion is indeed characterised by hyperdiffusion, $x \sim t^{2/3}$. Rather remarkably, independent of the underlying physical system the large-scale dynamic

processes obey identical hyper-diffusive dynamics. We also note that scaling of the form eq. (5) was found for the number of visits to the origin during a simulation (see in particular [18] Fig. 9).

Very similar phenomenology has recently been demonstrated in a lattice model, a lifted version of the widely studied simple exclusion process [19, 20]. This variant of TASEP was designed to mimic certain aspects of non-reversible Monte Carlo, in particular the paper [20] introduces a new backward transfer of the active particle inspired by the factor field construction from [18]. Here too, strong numerical evidence, via the Bethe ansatz, points to a non-trivial scaling of solutions involving $t^{2/3}$, without giving access to scaling functions. We conclude that this unusual scaling in time is observed in a wide variety of physical models (with very different underlying interactions) undergoing non-reversible dynamics subject to balance, without detailed balance.

Argument for algorithmic optimality

We note that motion $x \sim t^{2/3}$ is optimal for sampling via a single tracer particle (we do not consider algorithms involving global updates) leading to complete resampling of the modes of a one-dimensional system: Consider a section of l elements within a system of particles. Peierls argument, [21], tells us that the fluctuations in this section increase as $|\Delta l| \sim l^{1/2}$. After the algorithm that has been run for t steps to sample the system, activity has progressed $|x| \sim t^{\alpha}$. Thus, length fluctuations, if the section is fully re-equilibrated, are $|\Delta l| \sim t^{\alpha/2}$. From eq. (8) we see that the number of visits to the starting point of the simulation is $L(t,0) \sim t^{1-\alpha}$. If we identify the two expressions for the displacement then $t^{1-\alpha} \sim |\Delta l| \sim t^{\alpha/2}$, or $\alpha = 2/3$. Thus the amplitude of fluctuations, needed to re-equilibrate the section, is comparable to the number of returns of the algorithm to the origin, and thus the maximum displacement that can be generated for the origin in the time t.

Self-repelling motion and non-reversible simulation

We now simulate with an event-chain Monte Carlo an elastic chain at temperature, $T = 1$, with harmonic springs of unit strength, starting with a zero-temperature configuration. For concreteness, the active particle moves in the $+x$ direction. The algorithm proposes, at each time step, a displacement of the active particle which is vetoed after motion by a distance $O(1)$. Consider now a section of the chain, of $l + 1$ sites of the system $[0, l]$, which has been uniformly stretched, after running the algorithm for some time. For this to have occurred, there must have been more visits to the site labelled l than to the site 0, for instance for l=4 the zig-zag trajectory (01234)(32)(1234)(3)(234)(34) generates a stretched chain with number of visits for each site, $L_i = [1, 2, 4, 6, \ldots]$. This stretching then influences the future motion of the active particle. Such a stretch leads to a higher veto rate for transfers of the activity to the left of the chain, opposite to the gradient in L_i. However, this is exactly the phenomenology of eq. (2). If the exact details of the local update rule are not crucial in the dynamics and some form of large-scale universality applies eqs. (2, 3) are clearly candidates for a coarse-grained description of the motion generated by event-chain Monte Carlo. In event-chain simulation in higher dimension, we understand that relative motion of particles leads to a heterogeneous buildup in stress which will then back-react on the motion of the active particle, leading to a very similar coupling

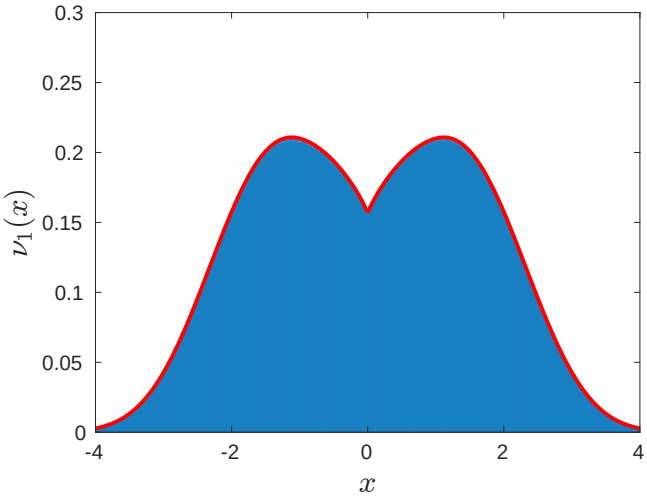

Figure 1. Scaling function for distribution, $\nu_1(x)$, eq. (6) curve in red, compared to simulation data where we have saved the index of the final point of a trajectory, blue histogram. The distribution is a function of only $|x|$, and is singular at $x = 0$. The empirical distribution has a standard deviation of $\sim 16,500$ sites.

of motion and history, though presumably the tensorial nature of stress in higher dimensions will change the exact mapping onto the self-avoiding walk.

Numerical results

Elastic chain

We generate data for the simulation of an elastic chain of N particles linked by harmonic springs. We initialise the chain to its ground state. We then perform $m = 134 \times 10^6$ simulations starting at the origin, $(i = 0)$ corresponding to $x = 0$ in the figures. Our simulated systems are periodic, but all simulations are too short in time to be influenced by the choice of a finite N, or to see wrap-around of trajectories. As is usual in event-driven Monte Carlo we simulate for an imposed chain length which we take here as $t = 10^6$. The mean-free path is slightly greater than unity, so this corresponds to very nearly 10^6 transfers of activity.

During each simulation, we cumulate the number of visits to each site by the active particle, in a manner analogous to eq (1) which we again denote $L_i(t)$. At the end of each of the m simulations we save the index of the final active particle (which in the continuum limit corresponds to a displacement x), as well as the number of visits of the active particle to the final chain position corresponding to the variable h of eq. (7). After the simulation, the data is binned generating empirical distributions, that we compare with eqs. (6, 7), see Figs. 1, 2. The red curves are the analytic results; blue shading corresponds to binned data from the Monte Carlo data. Fig. 1 corresponds to some 40,000 bins in the data, which give the appearance of a continuous curve. The curves represent probability distributions and are thus automatically normalized to unit area. The only free variable in comparing the analytic expressions to the binned numerical data is the choice of the horizontal scale. We fix this one scale by imposing that the first moment of the empirical curve matches the theoretical expression.

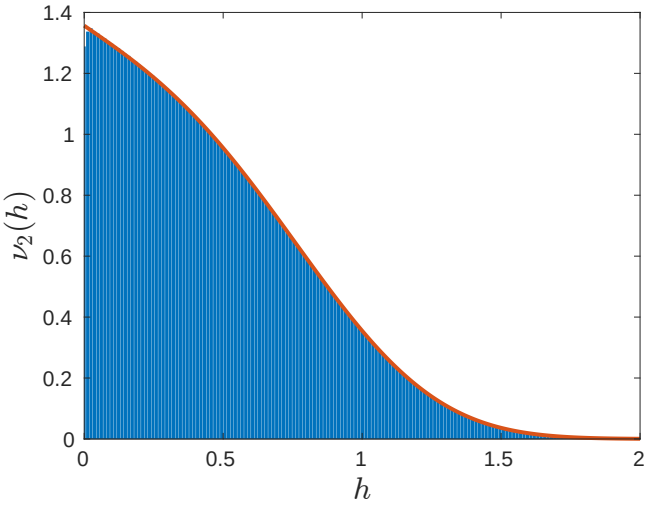

Figure 2. Scaling function for the number of site visits at the end-point of motion, $\nu_2(h)$ eq. (7) curve in red, compared to simulation data, blue histogram. Same simulation as Fig. 1

We find excellent agreement between theory and numerics. We note, in particular, that as predicted by theory the distribution of Fig. 1 has a singularity at the origin. The empirical curve, Fig. 2, for ρ_2 at $h = 0$ is systematically lower than the red, theoretical curve, this corresponds to simulations that finish on an as-yet unvisited site. This empirical curve, thus converges weakly to the theory, with the bar at $h = 0$ squeezed to zero width at the origin as t increases. We also performed simulations starting from a pre-equilibrated physical system. In this case, we find very similar distributions to those plotted in Figs. 1, 2 with however, a change of scale in the axes, see also [13].

Lifted TASEP

Finally, we perform a numerical study of the lifted TASEP model [20]. We consider a system of N particles on a periodic lattice of length $2N$. This new variant on the TASEP is a model of impenetrable particle motion on a lattice, in which collisions cause transfers of velocity. The modification in the calculation of [20] is the addition of a backward transfer of particle motion. For a special value of the backward transfer rate the lifted TASEP displays accelerated relaxation dynamics in density-density correlations in a manner which is similar to that displayed in continuum particle models[18]. We study this TASEP model only at this specific value of the backward rate where the dynamics is highly accelerated.

We initialise the system in a crystal of equally spaced particles. Simulations on short times give rise to an asymmetric distribution from for $\rho_1(x)$ (Fig. 3, top), but longer simulations give a very slow convergence to a more symmetric form (Fig. 3, bottom). We conclude that the lifted TASEP displays very similar phenomenology to the harmonic chain, and is also in the same dynamic universality class as true self-avoiding motion. We also confirmed, for lifted TASEP, the expected scaling of displacement of the activity in $t^{2/3}$, Fig. 4 (top). Fig. 4, (bottom) shows that

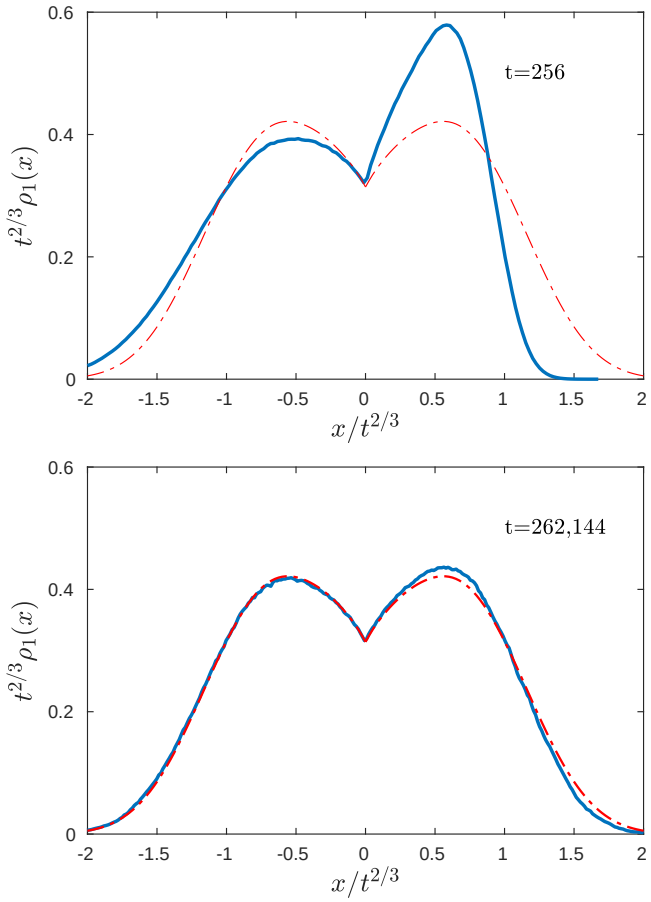

Figure 3. Distribution of displacements of the activity $\rho_1(t, x)$, for lifted TASEP. Top, a short simulation of $t = 256$ steps generates a skewed distribution. Bottom, a longer time scale of $t = 262,144$ generates a distribution which is close to that found in Fig. 1, while still displaying a very slight left-right asymmetry. Scaled curve of $\nu_1(x)$ red/dashed.

distribution of displacement is strongly skewed for short times; it is only after a long simulation that the back-forwards symmetry is established When we start with a configuration which is generated randomly, the initial asymmetry is weaker, though not zero.

Conclusions

To conclude, we have presented numerical evidence that the evolution of a system subject to non-reversible Monte Carlo is directly linked to the continuum limit of a growth model [7]. We performed extensive simulations using an event chain algorithm and compared the resulting distributions to those calculated in [12, 13, 22]. We find excellent agreement, for both a harmonic chain, and for the non-harmonic lifted TASEP, and so conclude that the non-reversible algorithm is indeed a realisation of a true self-repelling motion. We have shown that several *very different* physical systems

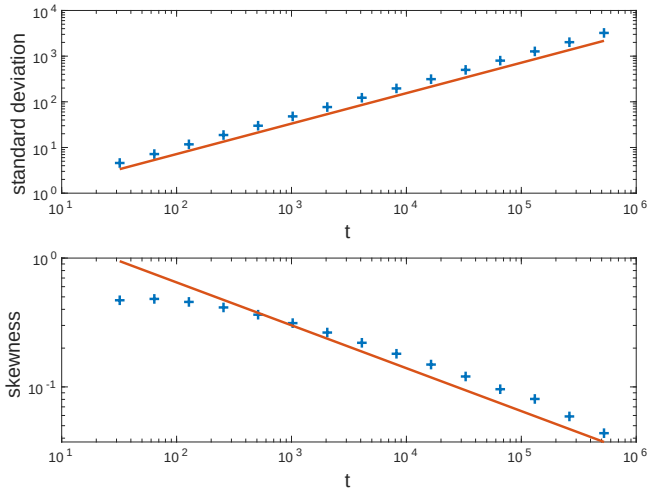

Figure 4. Evolution of moments of $\rho_1(t,x)$ for lifted TASEP. Top: standard deviation of the distribution, compared to evolution in $t^{2/3}$. Bottom, skewness (normalized third moment) compared to $t^{-1/3}$. The decrease in skewness corresponds to a distribution which progressively becomes more symmetric.

are members of the same dynamic universality class. It would be of great interest to understand why this is the case, and whether other systems display the same scaling behavior. As noted by [13] this universality class is distinct from KPZ (Kardar-Parisi-Zhang), even though similar special functions appear in the solutions.

Event-chain methods, including factor fields, have been generalized to higher dimensions [23]. It would be of interest to transfer the formalism of the present letter to such systems, perhaps using the approach of [24]. Applications in Monte Carlo simulation also require generalisations of the continuum equations to include extra, drift, terms due to coupling to external stresses [2].

The code used to simulate the two physical systems, as well as the plotting and analysis code is available from `https://github.com/acmaggs/Avoid`.

Acknowledgments

The author would like to thank Werner Krauth for extensive discussions on the subject of non-reversible simulation and lattice models.

References

[1] Bernard E P, Krauth W and Wilson D B 2009 *Phys. Rev. E* **80**(5) 056704 URL `https://link.aps.org/doi/10.1103/PhysRevE.80.056704`

[2] Michel M, Kapfer S C and Krauth W 2014 *The Journal of Chemical Physics* **140** 054116 ISSN 0021-9606 (*Preprint* `https://pubs.aip.org/aip/jcp/article-pdf/doi/10.1063/1.4863991/15472076/054116_1_online.pdf`) URL `https://doi.org/10.1063/1.4863991`

[3] Harland J, Michel M, Kampmann T A and Kierfeld J 2017 *Europhysics Letters* **117** 30001 URL `https://dx.doi.org/10.1209/0295-5075/117/30001`

[4] Faulkner M F, Qin L, Maggs A C and Krauth W 2018 *The Journal of Chemical Physics* **149** 064113 ISSN 0021-9606 (*Preprint* `https://pubs.aip.org/aip/jcp/article-pdf/doi/10.1063/1.5036638/13501056/064113_1_online.pdf`) URL `https://doi.org/10.1063/1.5036638`

[5] Kapfer S C and Krauth W 2015 *Phys. Rev. Lett.* **114**(3) 035702 URL https://link.aps.org/doi/10.1103/PhysRevLett.114.035702

[6] Bernard E P and Krauth W 2011 *Phys. Rev. Lett.* **107**(15) 155704 URL https://link.aps.org/doi/10.1103/PhysRevLett.107.155704

[7] Amit D J, Parisi G and Peliti L 1983 *Phys. Rev. B* **27**(3) 1635–1645 URL https://link.aps.org/doi/10.1103/PhysRevB.27.1635

[8] Bernasconi J and Pietronero L 1984 *Phys. Rev. B* **29**(9) 5196–5198 URL https://link.aps.org/doi/10.1103/PhysRevB.29.5196

[9] Pietronero L 1983 *Phys. Rev. B* **27**(9) 5887–5889 URL https://link.aps.org/doi/10.1103/PhysRevB.27.5887

[10] Obukhov S P and Peliti L 1983 *Journal of Physics A: Mathematical and General* **16** L147 URL https://dx.doi.org/10.1088/0305-4470/16/5/004

[11] Tóth B and Werner W 1998 *Probability Theory and Related Fields* **111** 375–452 URL https://doi.org/10.1007/s004400050172

[12] Tóth B 1995 *The Annals of Probability* **23** 1523 – 1556 URL https://doi.org/10.1214/aop/1176987793

[13] Dumaz L and Tóth B 2013 *Stochastic Processes and their Applications* **123** 1454–1471 ISSN 0304-4149 URL https://www.sciencedirect.com/science/article/pii/S0304414912002517

[14] Peliti L 1984 *Physics Reports* **103** 225–231 ISSN 0370-1573 URL https://www.sciencedirect.com/science/article/pii/037015738490084X

[15] *NIST Digital Library of Mathematical Functions* https://dlmf.nist.gov/, Release 1.1.11 of 2023-09-15 f. W. J. Olver, A. B. Olde Daalhuis, D. W. Lozier, B. I. Schneider, R. F. Boisvert, C. W. Clark, B. R. Miller, B. V. Saunders, H. S. Cohl, and M. A. McClain, eds. URL https://dlmf.nist.gov/

[16] Kapfer S C and Krauth W 2017 *Phys. Rev. Lett.* **119**(24) 240603 URL https://link.aps.org/doi/10.1103/PhysRevLett.119.240603

[17] Lei Z and Krauth W 2018 *Europhysics Letters* **121** 10008 URL https://dx.doi.org/10.1209/0295-5075/121/10008

[18] Lei Z, Krauth W and Maggs A C 2019 *Phys. Rev. E* **99**(4) 043301 URL https://link.aps.org/doi/10.1103/PhysRevE.99.043301

[19] Derrida B 1998 *Physics Reports* **301** 65–83 ISSN 0370-1573 URL https://www.sciencedirect.com/science/article/pii/S0370157398000064

[20] Essler F H L and Krauth W 2023 Lifted TASEP: a Bethe ansatz integrable paradigm for non-reversible Markov chains (*Preprint* 2306.13059)

[21] Peierls R 1935 *Annales de l'institut Henri Poincaré* **5** 177–222 URL http://www.numdam.org/item/AIHP_1935__5_3_177_0/

[22] Tóth B 2001 Self-interacting random motions *European Congress of Mathematics* ed Casacuberta C, Miró-Roig R M, Verdera J and Xambó-Descamps S (Basel: Birkhäuser Basel) pp 555–564 ISBN 978-3-0348-8268-2

[23] Maggs A C and Krauth W 2022 *Physical Review E* **105** URL https://doi.org/10.1103%2Fphysreve.105.015309

[24] Crane E, Ledger S and Tóth B 2019 *Journal of Statistical Physics* **177** 1240–1262 URL https://doi.org/10.1007/s10955-019-02419-9